

Effects of an Off-centered Tool on Multi-component Monopole and Dipole Logging

Joongmoo Byun and M. Nafi Toksöz

Earth Resources Laboratory
Department of Earth, Atmospheric, and Planetary Sciences
Massachusetts Institute of Technology
Cambridge, MA 02139

Abstract

Recent logging tools have monopole and dipole sources in one system, and the monopole and dipole components are acquired by adding or subtracting responses at four monopole (pressure) receiver arrays at right angles. We investigate the effects of tool eccentricity on this monopole receiver array system for three different eccentricity directions. To simulate responses at each receiver array, we use the discrete wavenumber method. An off-centered dipole source produces nondipole modes as well as the dipole mode and the responses detected at each receiver array have different features as eccentricity direction varies, showing the similar pattern for both fast and slow formation. We separate the modes included in a response and compare the amplitude of each mode to the other modes. By considering responses at each array separately, we can precisely resolve the effects associated with eccentricity direction.

1 Introduction

During a survey, the logging tool is normally kept on the axis of the borehole with the centralizers. However, it may not be possible to maintain the tool in perfect alignment in inclined, deviated, or horizontal boreholes. The source and receivers placed in off-axis or tilted position yield additional complexities, which can be obstacles to the interpretation of recorded logs. It is thus important to characterize the response of off-centered monopole and multipole sources.

Several studies have been done on the effects of off-centered sources and receivers. Roever et al. (1974) considered waves excited by centered and eccentric monopole sources in fluid-filled boreholes and showed laboratory scale model results. In 1982, Willis et al. evaluated the approximate effects of the off-centered tool and the tilted tool by using effective borehole radii and ray tracing. The effects of eccentric dipole sources were presented by Leslie and Randall (1990). They investigated changes in the amplitude and the estimated slowness of the flexural wave with eccentricity magnitude and orientation, formation slowness, and borehole radius. These changes are due to the interference of other nondipole ($n \neq 1$) components (e.g. monopole, quadrupole, etc.). Schmitt (1993) examined effects of an off-centered dipole source located in well-bonded and poorly bonded cased boreholes. For numerical simulation of eccentric dipole system, Leslie et al. and Schmitt used dipole source and dipole receivers (which record the radial displacement) by extending Kurkjian and Chang's (1986) formulation for centered ideal dipole sources to eccentric ones. In 1996, Zhang investigated the nonaxisymmetric acoustic fields excited by a cylindrical tool (monopole ring source) placed off the axis of a fluid-filled borehole. He presented a method of extraction of the shear wave from these nonaxisymmetric acoustic fields by subtracting two full waveforms logged at $\theta = 0$ and $\theta = \pi$.

New tools have been designed to produce monopole, dipole, and cross-dipole responses by using multi-component sources and receivers. One way to simulate the response from a dipole receiver is to place two monopole receivers (which record the pressure) at opposing sides of the logging tool (0° and 180°) and subtract the reception at one monopole receiver from that at the other. This receiver system can also simulate the response from a monopole receiver with two additional monopole receivers placed at 90° and 270° on the logging tool. The response for a monopole receiver is acquired by summing all receiver receptions. With this advantage, this monopole receiver system has been used for recent logging tools where one system contains both monopole and dipole sources.

In this paper, we investigate the acoustic fields generated and recorded by off-centered tools. We calculate the response of each monopole receiver separately by the discrete wavenumber method (Cheng and Toksöz, 1981; Tubman et al., 1984; Schmitt and Bouchon, 1985). Then, by combining these responses

through additions or subtractions, we synthesize monopole, dipole, and multipole logs. Emphasis is given to a dipole source in the presence of a slow formation. We examine individual modes contributing to the response of each receiver, and their amplitudes with different eccentricity directions. Finally, the advantage of using monopole receivers in analyzing the effects of an eccentric dipole source is discussed.

2 3D Wave Propagation Solution for a Fluid-filled Borehole

To evaluate the 3D field generated by an off-centered point pressure source in a fluid-filled borehole, we followed Tadeu's work (1992). Consider a cylindrical fluid-filled borehole buried in a homogeneous elastic medium of infinite extent. For a harmonic point pressure source at position $(x_0, 0, 0)$, oscillating with a frequency ω , the incidence field can be expressed by using dilatational potential ϕ :

$$\phi_{inc}(t, x, y, z) = \frac{A \exp \left[i \frac{\omega}{\alpha} \left(\alpha t - \sqrt{(x-x_0)^2 + y^2 + z^2} \right) \right]}{\sqrt{(x-x_0)^2 + y^2 + z^2}} \quad (1)$$

where A is the wave amplitude, α is the compressional wave velocity of the fluid containing the source, and $i = \sqrt{-1}$.

Defining the effective wavenumbers

$$k_\alpha = \sqrt{\frac{\omega^2}{\alpha^2} - k_z^2}, \quad \text{Im } k_\alpha < 0 \quad (2)$$

$$k_\beta = \sqrt{\frac{\omega^2}{\beta^2} - k_z^2}, \quad \text{Im } k_\beta < 0$$

with the axial wavenumber, k_z , and Fourier transforming equation (1) in the z direction, one obtains

$$\phi_{inc}(\omega, x, y, k_z) = \frac{-iA}{2} H_0^{(2)} \left(k_\alpha \sqrt{(x-x_0)^2 + y^2} \right) \quad (3)$$

where the $H_n^{(2)}(\dots)$ are the Hankel functions of the second kind and order n . However, equation (3) expresses the incident field in terms of waves centered at the source point $(x_0, 0, 0)$, and not at the axis of the borehole. By Graf's addition theorem (Watson, 1980), the incident potential in equation (3) can be rewritten in terms of waves at the origin in the cylindrical coordinates:

$$\phi_{inc}(\omega, r, \theta, k_z) = \frac{-iA}{2} \sum_{n=0}^{\infty} (-1)^n \varepsilon_n H_n^{(2)}(k_\alpha r_0) J_n(k_\alpha r) \cos(n\theta) \quad (4)$$

when $r < r_0$

$$\phi_{inc}(\omega, r, \theta, k_z) = \frac{-iA}{2} \sum_{n=0}^{\infty} (-1)^n \varepsilon_n H_n^{(2)}(k_\alpha r) J_n(k_\alpha r_0) \cos(n\theta) \quad (5)$$

when $r > r_0$

where the $J_n(\dots)$ are Bessel functions of order n , θ is the azimuth, and

$$\varepsilon_n = \begin{cases} 1 & \text{if } n = 0 \\ 2 & \text{if } n \neq 0 \end{cases}$$

$r = \sqrt{x^2 + y^2}$ is the radial distance to the receiver,

r_0 is the radial distance from the cylindrical axis to the source, and

$\cos \theta = x/r$, $\sin \theta = y/r$.

In the (ω, k_z) domain, the scattered fields in the solid formation can be written in a similar form to that of the incident field:

$$\phi_{sca}^s(\omega, r, \theta, k_z) = \sum_{n=0}^{\infty} A_n H_n^{(2)}(k_\alpha r) \cos(n\theta)$$

$$\psi_{sca}^s(\omega, r, \theta, k_z) = \sum_{n=0}^{\infty} B_n H_n^{(2)}(k_{\beta_s} r) \sin(n\theta) \quad (6)$$

$$\chi_{sca}^s(\omega, r, \theta, k_z) = \sum_{n=0}^{\infty} C_n H_n^{(2)}(k_{\beta_s} r) \cos(n\theta)$$

where ψ and χ are shear potentials which satisfy a wave equation with a shear wave velocity β . A_n , B_n , and C_n are unknown coefficients to be determined from appropriate boundary conditions. Index s indicates that the wave velocities of the *solid* formation must be used. The scattered field in the fluid can be expressed as

$$\phi_{sca}^f(\omega, r, \theta, k_z) = \sum_{n=0}^{\infty} D_n J_n(k_{\alpha_f} r) \cos(n\theta) \quad (7)$$

where index f indicates the fluid, and

$$k_{\alpha_f} = \sqrt{\frac{\omega^2}{\alpha_f^2} - k_z^2}.$$

D_n is also determined from boundary conditions. The total field inside the borehole fluid is the sum of the incident field and the scattered field in the fluid:

$$\phi_{tot} = \phi_{inc} + \phi_{sca}^f \quad (8)$$

3 Constructing Multipole Sources and Acquiring Multipole Components

Kurkjian and Chang (1986) showed that a multipole source of order n could be constructed from $2n$ monopoles (point sources) placed in the same horizontal plane. The monopoles are positioned periodically along the circle and alternate in sign. In addition, they pointed out that an array of pressure sensors on the axis of the borehole would only sense the monopole component of an acoustic field. They concluded that a sensor which responds to the n^{th} radial derivative of the displacement potential would sense only the n^{th} order multipole component of the acoustic field in the borehole. That is, we need to deploy an array of horizontal displacement sensors on the axis of the borehole to receive the dipole component of an acoustic field, and we need the spatial derivative of displacement for quadrupole component.

In a multi-component source and receiver system, the dipole source is constructed of two point sources of opposite sign (Figure 1b) and quadrupole source is constructed of four point sources of alternate sign at right angles to each other (Figure 1c). A monopole source can be implemented by four point sources of the same sign (Figure 1a). The monopole and multipole components can be acquired by subtracting or adding the responses at four receivers. If we call responses at receiver arrays A, B, C, and D depending on their locations associated with point sources as shown in Figure 1, the dipole component can be obtained by A-C, the quadrupole component by A-B+C-D, and the monopole component by A+B+C+D.

Figure 2 shows traces and phase velocities of the modes in the monopole component with a monopole source, the dipole component with a dipole source, and the quadrupole component with a quadrupole source, which were all obtained by the above methods. Tools were positioned on the axis of a fluid-filled borehole surrounded by a slow formation. The diameter of the borehole was 0.2032 m. The compressional and shear wave velocities of the formation were 2000 m/s and 1000 m/s, respectively, and the density was 2.0 g/cm³. The velocity of the fluid inside the borehole was 1500 m/s and its density was 1.0 g/cm³. Each receiver array had eight receivers spaced at 0.1524 m. The offset between the first receiver and the source was 2.4384 m. To acquire synthetic waveforms at receivers, we computed the responses in the frequency range from 0 to 10 kHz. For a source wavelet, a Ricker wavelet with a center frequency of 1.5 kHz was used. The phase velocities of the modes were obtained by Nolte et al.'s method (1997). As shown in the figure, the dispersion curves of the modes agree with the Stoneley mode (Figure 2a), the flexural mode (Figure 2b), and the screw mode (Figure 2c). There is the deviation in the low frequency in Figure 2c, but this frequency range is below the cutoff frequencies of the screw mode (about 3000 Hz). Therefore, we see that when a tool is placed at the center, we can obtain the monopole mode from A+B+C+D with a monopole source, the dipole mode from A-C with a dipole source, and the quadrupole mode A-B+C-D with a quadrupole source. In all cases, refracted P waves were observed, but they are not

shown in the figure due to scaling of the plots. The arrivals of refracted P waves are indicated by dotted lines.

The response at each receiver was examined separately. The response A in each case is depicted in Figure 3 as an example. When the source was a dipole, both A and C responses from receivers in line with a dipole source included only the flexural wave ($n = 1$). Because the flexural wave in A had the opposite polarity to that in C, the flexural wave was more enhanced by subtraction. In contrast, B and D responses from receivers perpendicular to the dipole direction were zero. Therefore, B-D, which corresponds to the response at the dipole receiver perpendicular to the dipole direction, was also zero. From the above observation, we can infer that A+B+C+D and A-B+C-D will yield zero responses. When the source was a quadrupole, only the screw wave ($n = 2$) appeared at all responses (A, B, C, and D). Since the polarities of A and C were the same and opposite to those of B and D, this screw wave was enhanced by A-B+C-D. However, A-C or A+B+C+D will produce zero response in this case. With a monopole source, only the Stoneley ($n = 0$) waves were observed at all receivers. They had the same amplitude and polarities. Thus A+B+C+D enhanced the Stoneley wave, while A-C and A-B+C-D will yield zero responses. Note that we can only obtain the $n = 0$ mode with a monopole source, only the $n = 1$ mode with a dipole source, and only the $n = 2$ mode with a quadrupole source if a tool is placed at the center of the borehole. In all the above cases, when the response is not zero, a refracted P wave was also present. Because the polarity of the refracted P wave was the same as of the mode component, it was also enhanced through the combination of the responses. Because we are interested in modal components, we will exclude refracted P and S waves from future discussion. If there is no specific comment, we will assume a refracted P wave exists in the response for the slow formation case and refracted P and S waves exist in the response for the fast formation case.

4 Off-centered Dipole Source

Considering eccentricity direction, three eccentric dipole sources were investigated and compared to a centric dipole source. The locations of the source-receiver assembly in three eccentric cases are shown in Figure 4. In all eccentric dipole cases, receivers were moved to the same direction as the source by the same radial displacement 0.03874 m (38% of the borehole radius). In the ‘Off 0’ case and the ‘Off 90’ case, the source and receivers were moved toward the array A and D, respectively. In the ‘Off 45’ case, the source and receivers were moved to the middle between the array A and D. Except for the radial locations of the source and receivers, the other geometrical parameters and formation properties were the same as the centric dipole source case in the previous section.

Figure 5 shows traces and phase velocities of the modes in A-C of three eccentric cases with a centric case (shown in Figure 2b). Traces in eccentric cases look similar to those in the centric case, but the dispersion curves are deviated from the centric case, especially around 1500 Hz. This deviation was produced by the nondipole ($n \neq 1$) modes because an off-centered dipole source produces the nondipole modes as well as the dipole (flexural) mode (Leslie and Randall, 1990).

4.1 Modal Analysis

For the precise interpretation of the log data, it is worth investigating which nondipole mode has the most effect on the data in an eccentric case. From the equations (6) and (7), we can see that the reflected (scattered) waves from an off-centered source are constructed from the contributions of infinite numbers of multipole modes with different orders. Thus, we can divide the reflected field into the monopole mode ($n = 0$), the dipole mode ($n = 1$), the quadrupole mode ($n = 2$), and higher modes ($n > 2$) depending on n . In this section, we extract each mode from the acoustic field excited by an off-centered dipole source, then we compare their contributions to the responses of each receiver array. The responses at monopole receiver arrays, A, B, C, D, and their combinations, A-C (in-line dipole receiver), B-D (cross dipole receiver), A+B+C+D, and A-B+C-D are considered without direct waves. Because the contributions of the modes higher than the quadrupole mode ($n > 2$) are very small, only $n = 0, 1, \text{ and } 2$ modes are displayed, except for a case of the source with 8 kHz center frequency.

The modes $n = 0, 1, \text{ and } 2$ included in the responses of the centric case are shown in Figure 6. We can confirm that a dipole source placed at the borehole axis yields only the dipole mode. The responses B, D, B-D, A+B+C+D, and A-B+C-D are zero.

In the Off 0 case (Figure 7), the dipole mode ($n = 1$) is contaminated by the nondipole modes. The Stoneley modes have the greatest amplitude in the responses at all monopole receiver arrays. Especially, the Stoneley mode is dominant in C at the receiver that is positioned close to the borehole axis. However, after subtracting C from A, the flexural wave becomes more dominant in A-C because the amplitude of the Stoneley waves in A and C are similar and thus, they are significantly reduced by subtraction. The amplitude of the Stoneley wave decays from the borehole wall to the borehole axis, and its decay rate decreases with decreasing frequency. The responses B and D are no longer zero in this case. However, B-D is zero because responses B and D are equal. By summing all receiver responses (A+B+C+D), the $n = 0$ mode is enhanced. Although the quadrupole mode ($n = 2$) makes little contribution to the responses at receivers except for A, it is enhanced in A-B+C-D.

Similar to the Center case, only responses at receivers in line with the dipole source (A and C) are not zero in the Off 90 case (Figure 8). The flexural mode is the dominant response, but there are also the quadrupole mode and higher modes ($n > 2$), unlike the Center case. Note that there is no monopole mode ($n = 0$). The responses B and D are zero, therefore B-D is zero. Note that the Off 0 case and the Off 90 case can be easily distinguished from each other by examining B and D, even though their cross-dipole responses, B-D, show zero for both cases. The response A+B+C+D and A-B+C-D are zero.

In the Off 45 case (Figure 9), the nondipole modes and the dipole mode appear at all receivers. However, by A-C, the dipole mode is enhanced. In addition, A+B+C+D and A-B+C-D enhance the monopole mode and the quadrupole mode, respectively.

The results with a 1.5 kHz center frequency source indicate that the Stoneley mode is the strongest nondipole mode when a dipole source is off-centered. Figure 10 shows the phase velocities of the modes shown in Figure 5b and 5d with the dispersion curve of the Stoneley mode. We can see that the deviation from the dispersion curve of the flexural mode around 1.5 kHz came from the effect of the Stoneley mode.

4.2 Source with 8 kHz Center Frequency

The responses show similar patterns to those with a 1.5 kHz source except for a few differences. In this case the amplitude of the refracted P waves are comparable to the interface modes, and the contribution of the $n = 3$ mode cannot be ignored. The dipole modes are the strongest modes in the responses except for the response (C in the Off 0 case) from the receiver closest to the borehole axis. Moreover, the amplitude of the Stoneley wave rapidly decayed from the borehole wall to the center. In responses A-C and A-B+C-D, the dipole mode and the quadrupole mode are enhanced, respectively, in Off 0 and Off 45 cases. However, the dipole mode is still dominant in A+B+C+D in both cases. Figure 11 shows the responses in the Off 0 case.

4.3 Fast Formation with a Source of 1.5 kHz Center Frequency

For a fast formation, 4210 m/s and 2655 m/s are used for the compressional and shear wave velocities, respectively, and the density is 2.14 g/cm³. The fluid velocity is 1500 m/s and the density is 1.0 g/cm³. The responses for the fast formation show similar patterns to those for the slow formation except that the refracted S waves and pseudo-Rayleigh waves exist. In addition, the amplitude of the quadrupole mode is very small compared to the monopole and the dipole modes. The dipole mode is still dominant in the response A-B+C-D for the Off 0 and the Off 45 cases.

5 Conclusions

With four monopole receiver arrays at right angles, we can acquire the monopole component by adding all responses (A+B+C+D), the dipole component by subtracting responses at in-line receiver arrays (A-C), and the quadrupole component by A-B+C-D. When a source is at the axis of the borehole, we can obtain only the monopole mode with a monopole source, only the dipole mode with a dipole source, and only the quadrupole mode with a quadrupole source.

Acoustic fields excited from an eccentric dipole source were examined with this four-monopole receiver array system. By subtracting the response from opposing receivers, we can obtain the responses corresponding to in-line and cross-line dipole receivers. Three eccentric dipole source cases were investigated with different eccentricity directions: in-line direction of the dipole source (Off 0 case), cross-line direction (Off 90 case), and 45 degrees to the dipole source (Off 45 case).

For precise analyses, modes included in the responses were extracted separately and the amplitude of each mode was compared to the other modes. When the dipole source was placed at the center, the in-line receiver arrays (A and C) have only the flexural mode while the cross receiver arrays (B and D) have no response. However, as the dipole source moved from the center, nondipole modes are generated. In Off 0 case, responses B and D have modes with the same amplitudes and polarities. The Off 0 case can be distinguished from Off 90 case, where responses B and D are zero. The responses A and C in the Off 90 case included the quadrupole ($n = 2$) mode and the higher modes ($n > 2$), although the dipole mode is dominant as in the Center case. An off-centered, low frequency dipole source with a center frequency of 1.5 kHz excited a strong Stoneley mode except for the Off 90 case. However, the amplitude of the Stoneley mode did not vary rapidly inside the borehole, and it was significantly reduced by A-C.

When the center frequency of an off-centered dipole source was 8 kHz, the dipole mode became the biggest mode in the responses except for receivers close to the borehole axis. The amplitude of the Stoneley mode was prominently changed with the position inside the borehole.

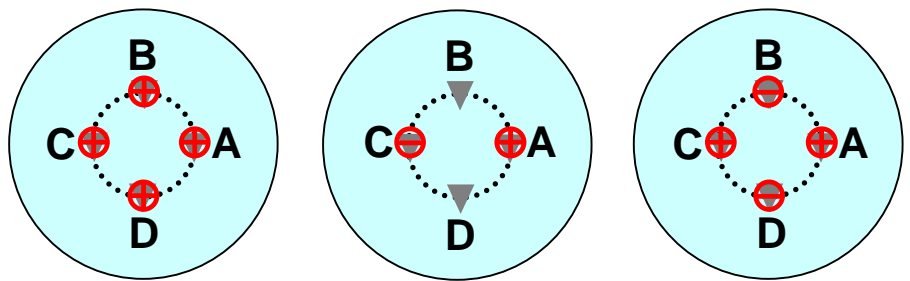
For all cases with a dipole source, the dipole mode was enhanced by A-C. However, enhancement of the monopole and the quadrupole component by A+B+C+D and A-B+C-D with a dipole source was not always guaranteed depending on the source frequency and the formation properties.

6 Acknowledgements

This work was supported by the MIT Earth Resources Laboratory's Founding Member Consortium, and the Borehole and Acoustic Logging Consortium.

References

- Cheng, C. H., and , Toksöz, M. N., 1981, Elastic wave propagation in a fluid filled borehole and synthetic acoustic logs: *Geophysics*, **46**, 1042-1053.
- Kurkjian, A., and Chang, S. K., 1986, Acoustic multipole sources in fluid-filled boreholes: *Geophysics*, **51**, 148-163.
- Leslie, H. D., and Randall, C. J., 1990, Eccentric dipole sources in fluid-filled boreholes - Numerical and experimental results: *J. Acoust. Soc. Am.*, **87**, 2405-2421.
- Nolte, B., Rao, R. V. N., and Huang, X., 1997, Dispersion analysis of split flexural waves: M.I.T. Borehole Acoustics and Logging and Reservoir Delineation Consortia Annual Report.
- Roever, W. L., Rosenbaum, J. H., and Vining, T. F., 1974, Acoustic waves from an impulsive source in a fluid-filled borehole: *J. Acoust. Soc. Am.*, **55**, 1144-1157.
- Schmitt, D., 1993, Dipole logging in cased boreholes: *J. Acoust. Soc. Am.*, **93**, 640-657.
- Schmitt, D., and Bouchon, M., 1985, Full-wave acoustic logging: Synthetic microseismogram and frequency-wavenumber analysis: *Geophysics*, **50**, 1756-1778.
- Tadeu, A. J. B., 1992, Modeling and seismic imaging of buried structures: Ph.D. Thesis, Massachusetts Institute of Technology.
- Tubman, K. M., Cheng, C. H., and , Toksöz, M. N., 1984, Synthetic full-waveform acoustic logs in cased boreholes: *Geophysics*, **49**, 1051-1059.
- Watson, G. N., 1980, A treatise on the theory of Bessel function: Cambridge University Press, Second Edition.
- Willis, M. E., Toksöz, M. N., and Cheng, C. H., 1982, Approximate effects of off-Center acoustic sondes and elliptic boreholes upon full waveform logs: *52nd Ann. Internat. Mtg., Soc. Expl. Geophys.*, Expanded Abstracts, 321-322.
- Zhang, B., 1996, Nonaxisymmetric acoustic field excited by a cylindrical tool placed off a borehole axis and extraction of shear wave: *J. Acoust. Soc. Am.*, **99**, 682-690.



(a) Monopole source (b) Dipole source (c) Quadrupole source

⊕ ⊖ : Positive and negative point sources ▼ : Receiver array
A, B, C, and D: positions of receiver arrays

Figure 1: Construction of a monopole, dipole, and quadrupole source with point sources.

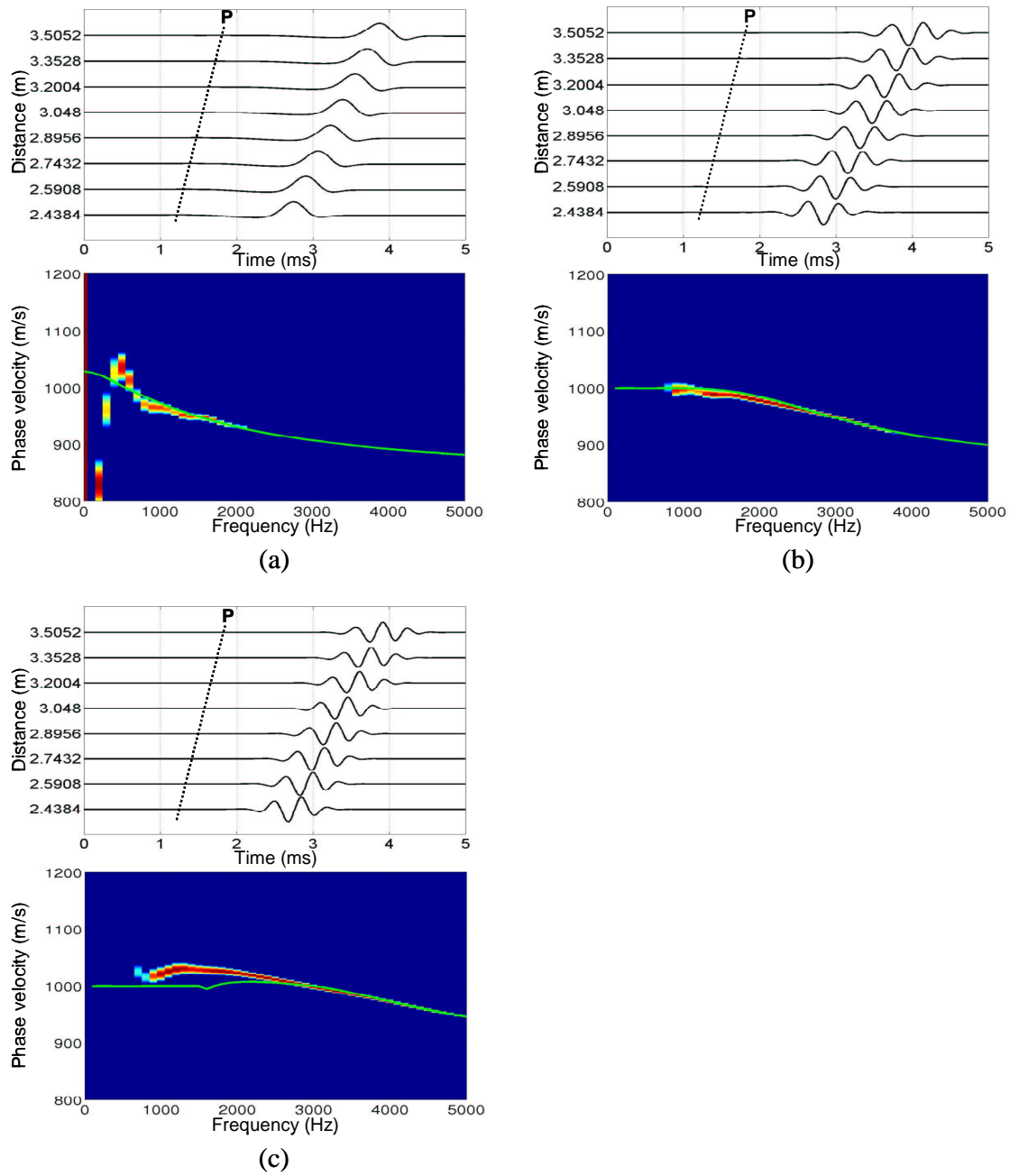


Figure 2: Traces and phase velocities of the modes obtained by Nolte et al.'s method (1997). Green lines are the theoretical dispersion curves of (a) the Stoneley mode, (b) the flexural mode, and (c) the screw mode. Dotted lines indicate the arrivals of refracted P waves.

- (a) A+B+C+D with a monopole source.
- (b) A-C with a dipole source.
- (c) A-B+C-D with a quadrupole source.

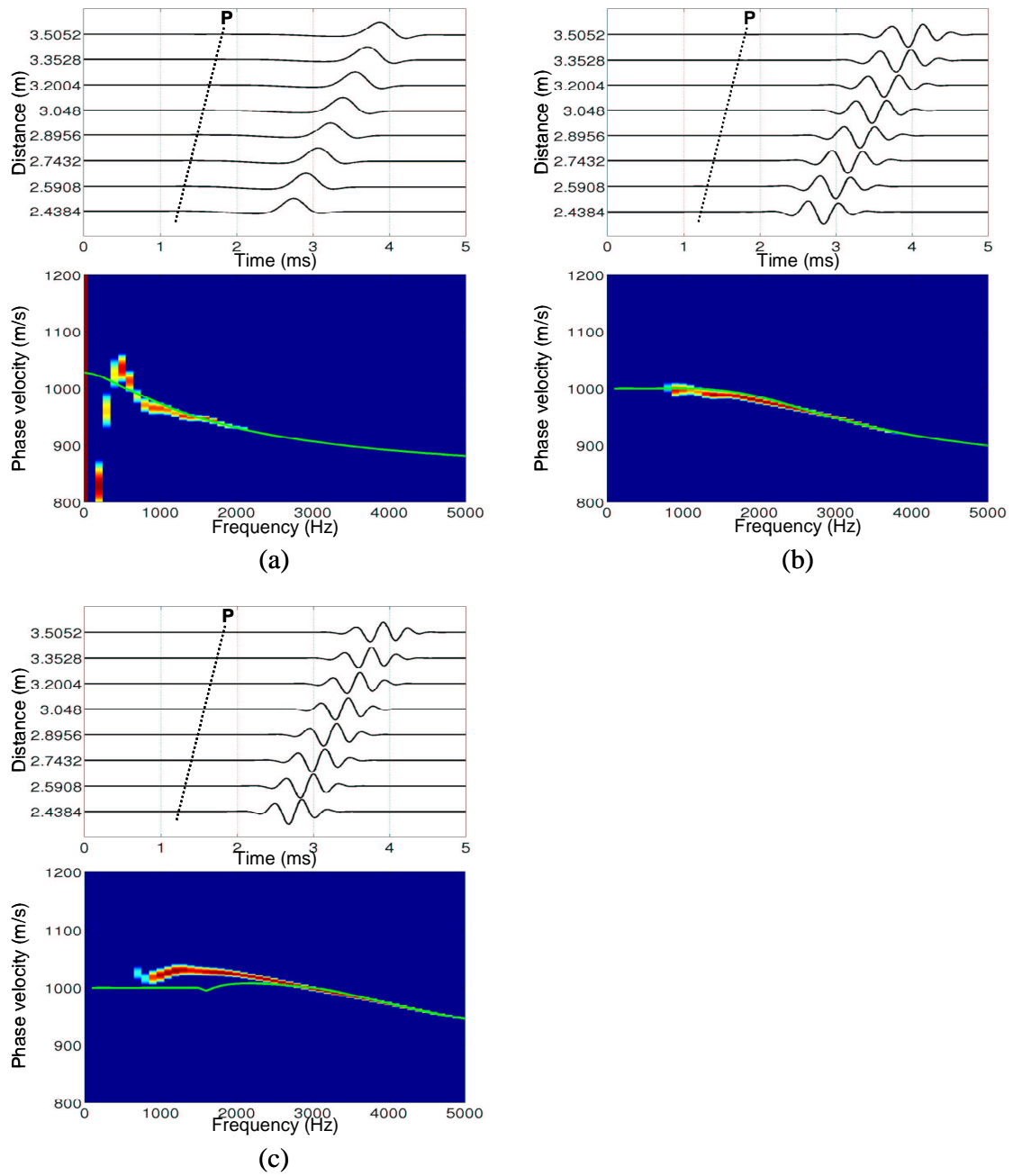


Figure 3: Traces and phase velocities of the modes obtained by Nolte et al.'s method (1997). Green lines are the theoretical dispersion curves of (a) the Stoneley mode, (b) the flexural mode, and (c) the screw mode. Dotted lines indicate the arrivals of refracted P waves.

- (a) A with a monopole source.
- (b) A with a dipole source.
- (c) A with a quadrupole source.

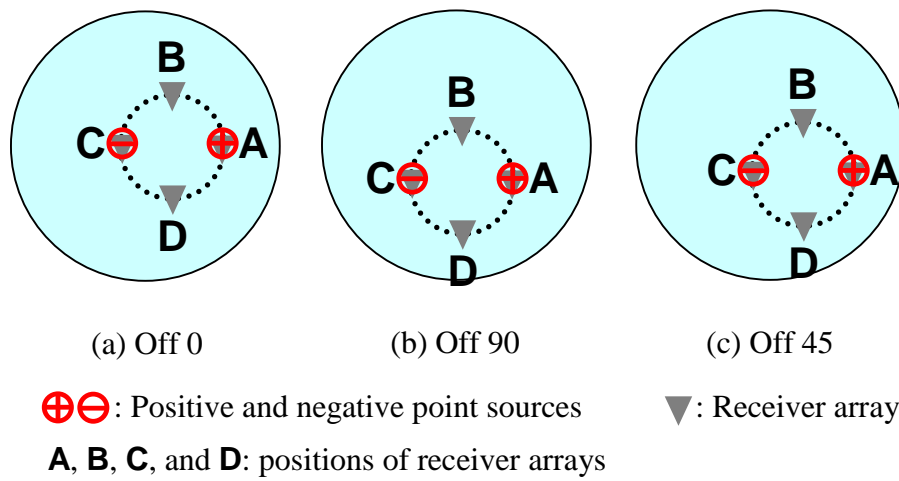


Figure 4: The configuration of the source-receiver assembly and its locations in three eccentric cases.

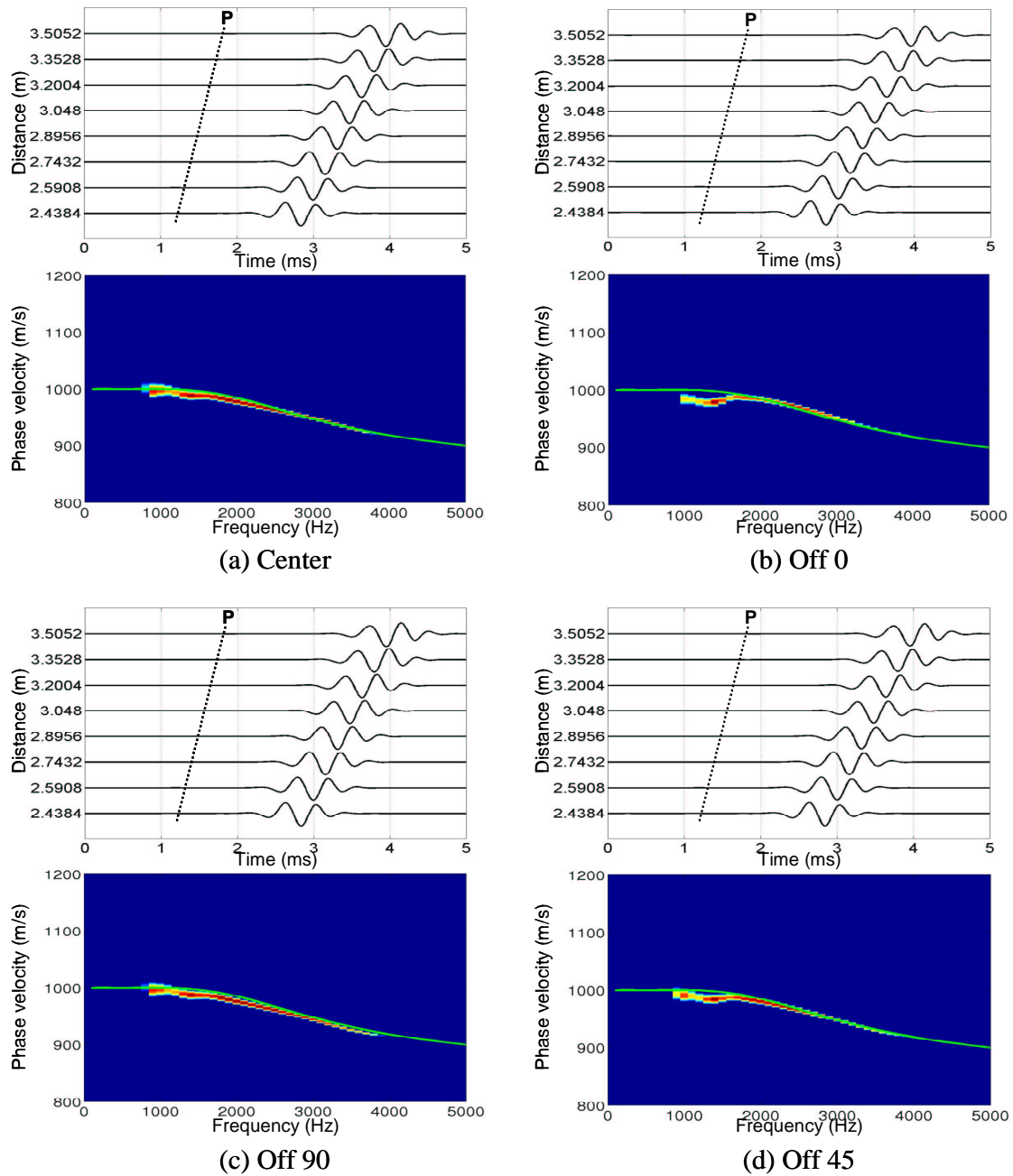
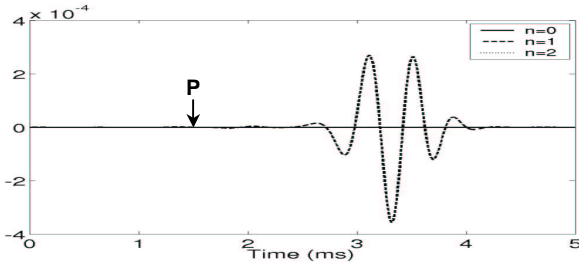
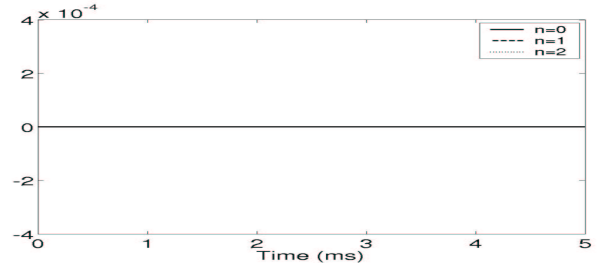


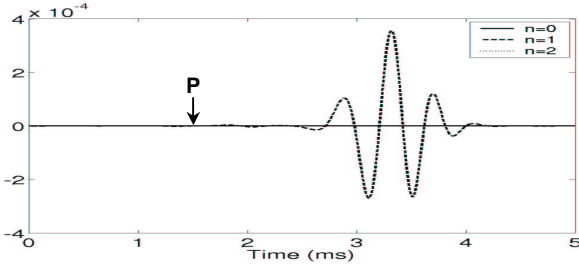
Figure 5: Traces and frequency semblance plots of A – C responses. Green lines are the dispersion curves of the flexural waves from dispersion analysis.



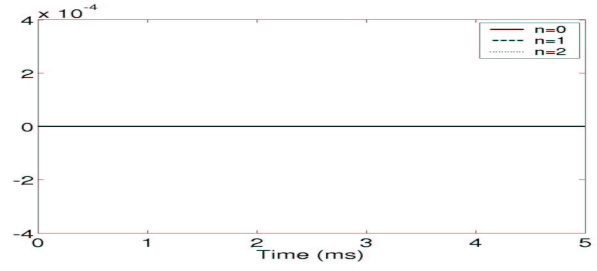
(a) A



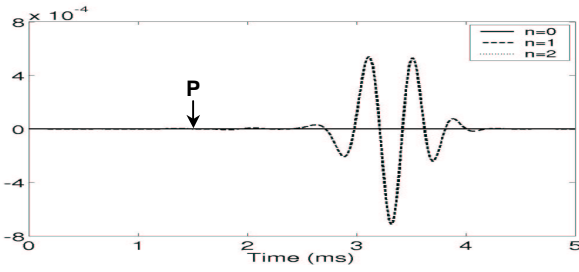
(b) B



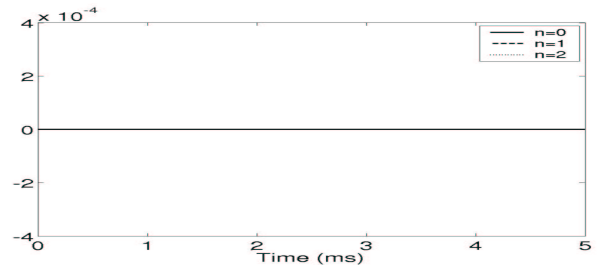
(c) C



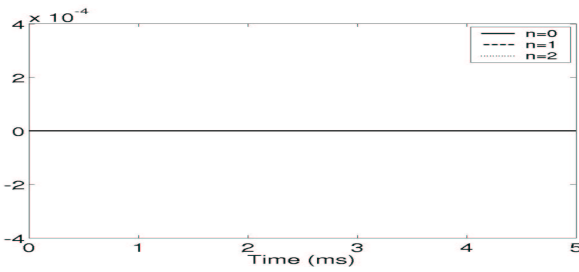
(d) D



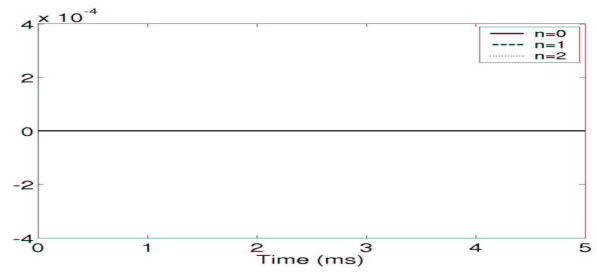
(e) A-C



(f) B-D



(g) A+B+C+D



(h) A-B+C-D

Figure 6: Modal components ($n = 0,1,2$) received at 2.8956 m away from a dipole source at the axis of the borehole.

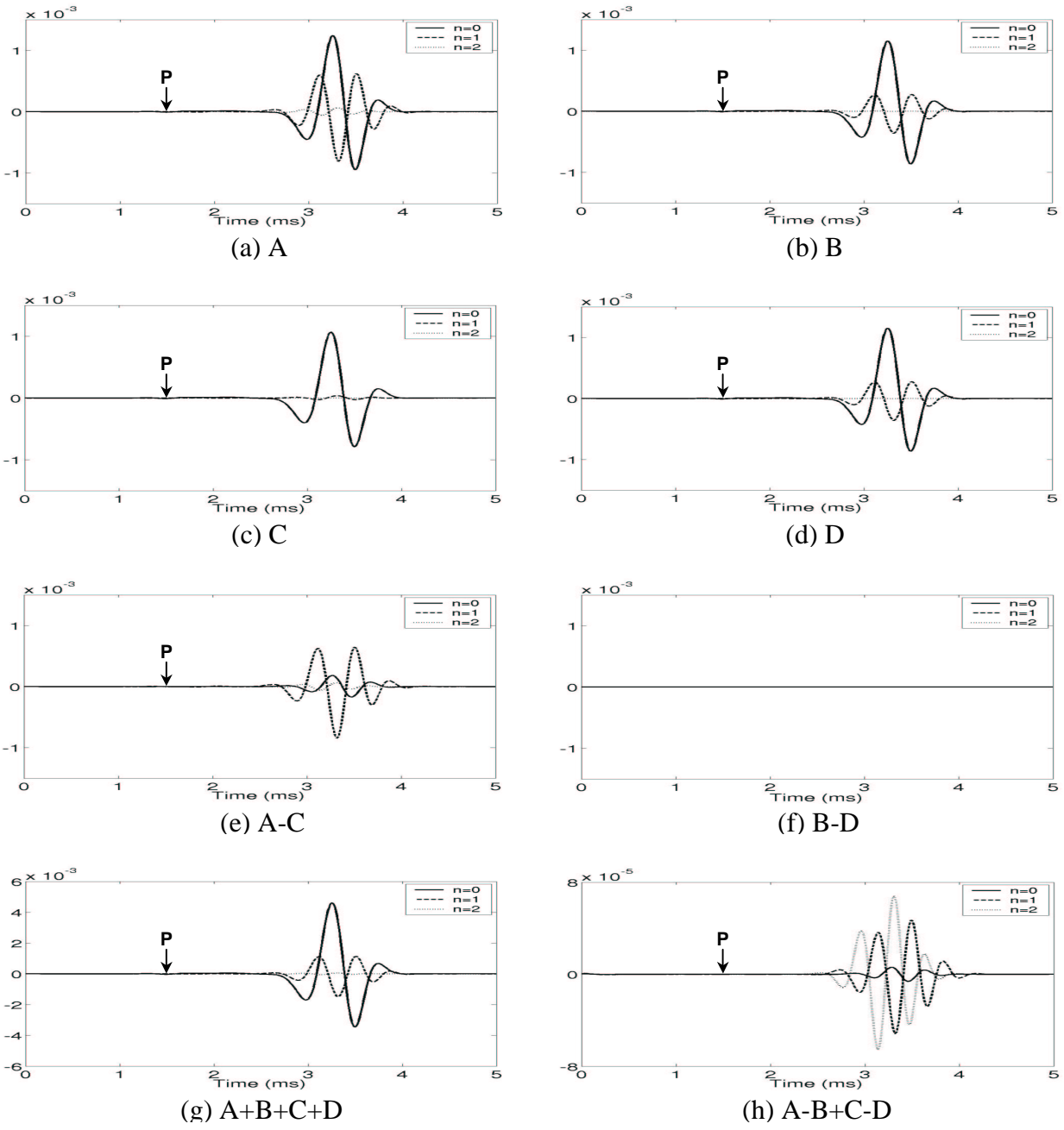
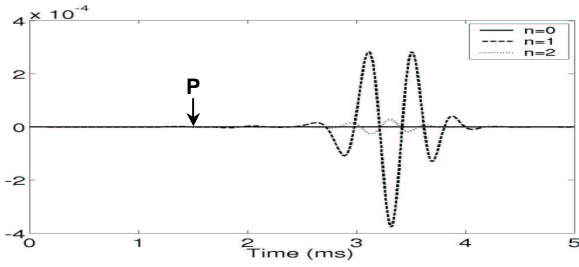
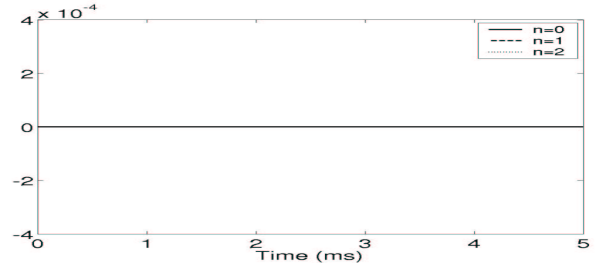


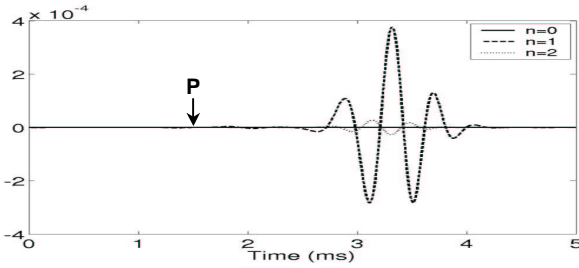
Figure 7: Modal components ($n = 0, 1, 2$) received at 2.8956 m away from an off-centered dipole source (Off 0).



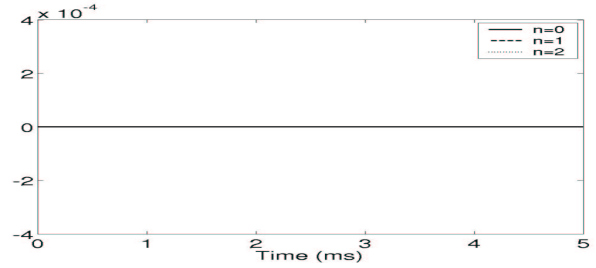
(a) A



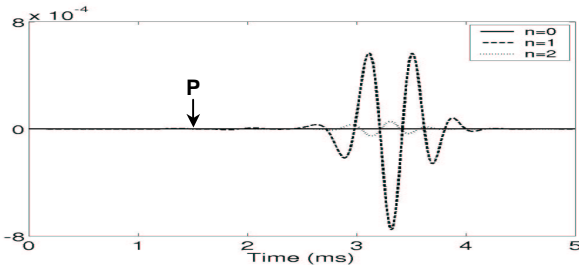
(b) B



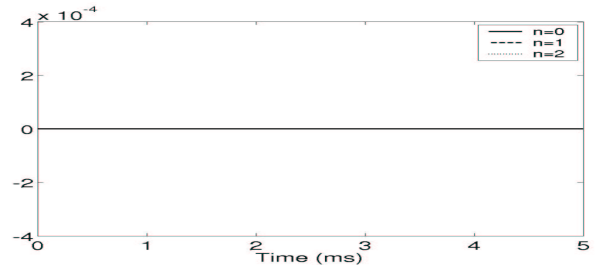
(c) C



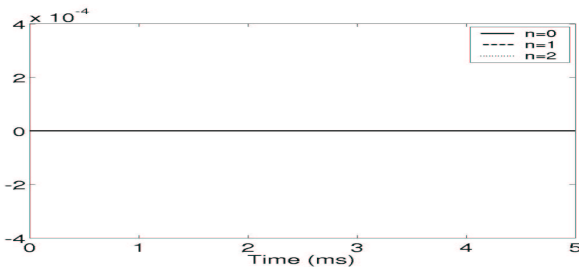
(d) D



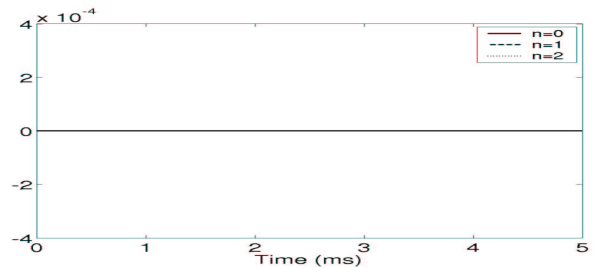
(e) A-C



(f) B-D



(g) A+B+C+D



(h) A-B+C-D

Figure 8: Modal components ($n = 0, 1, 2$) received at 2.8956 m away from an off-centered dipole source (Off 90).

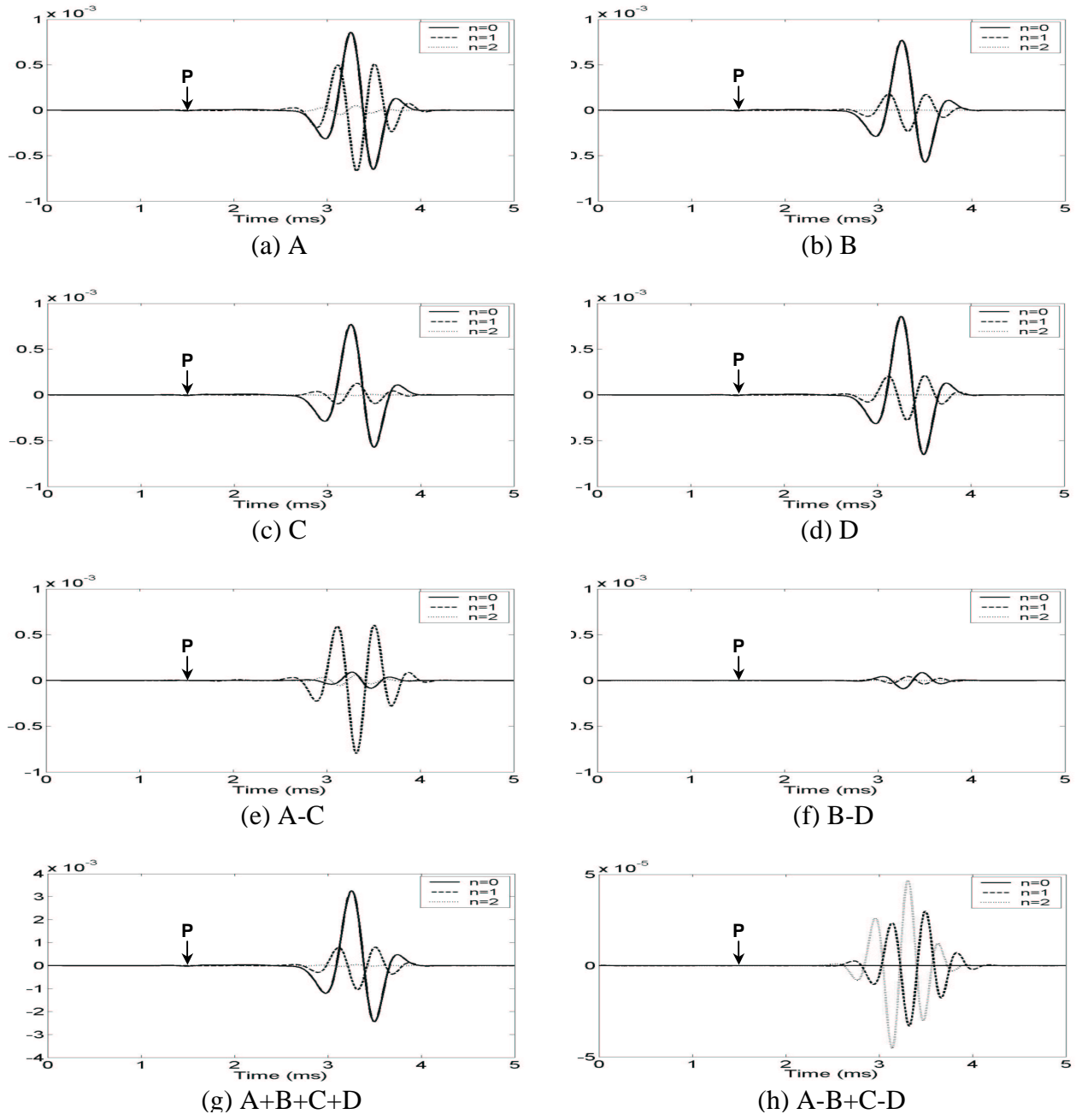
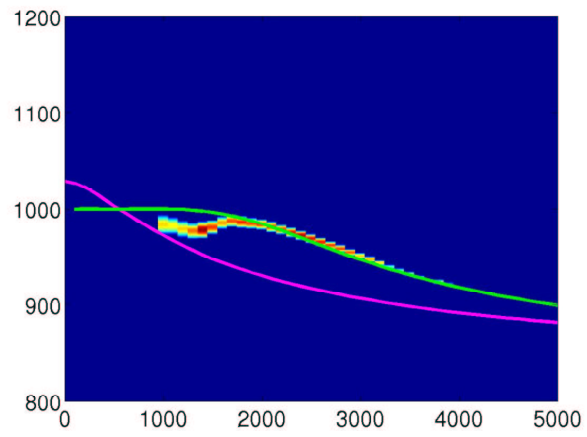
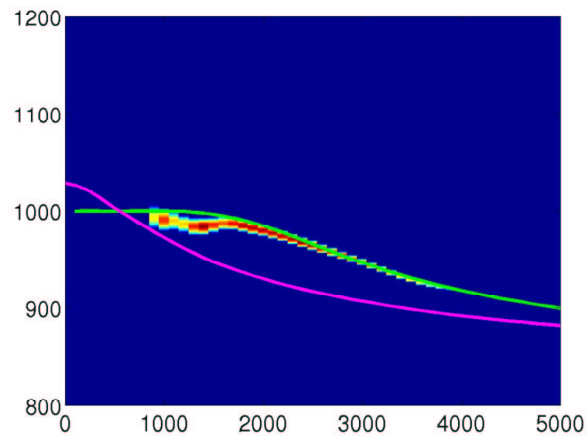


Figure 9: Modal components ($n = 0, 1, 2$) received at 2.8956 m away from an off-centered dipole source (Off 45).



(a)



(b)

Figure 10: The phase velocities of A – C responses (a) for the Off 0 case and (b) for the Off 45 case. Green lines are the dispersion curves of the flexural waves and pink lines are the dispersion curves of the Stoneley waves from the dispersion analysis.

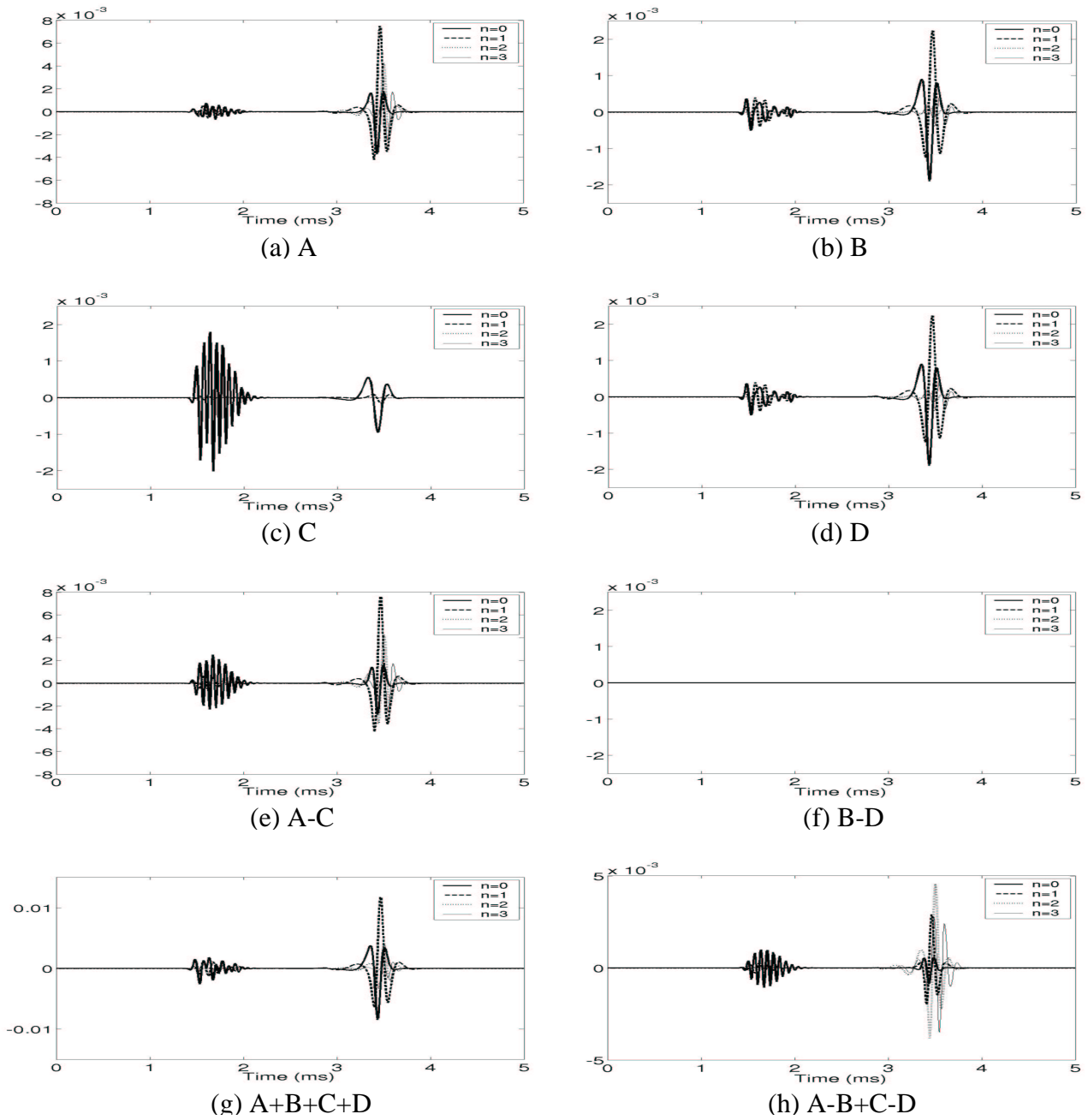


FIG. 11. Modal components ($n = 0, 1, 2$) received at 2.8956 m away from an off-centered dipole source (Off 0). The center frequency of the dipole source is 8 kHz.